

Solution-combustion synthesis of $\text{Bi}_{1-x}\text{Ln}_x\text{O}_{1.5}$ ($\text{Ln} = \text{Y}$ and La–Yb) oxide ion conductors

MANJUNATH B BELLAKKI, A S PRAKASH, C SHIVAKUMARA, M S HEGDE* and A K SHUKLA[†]

Solid State and Structural Chemistry Unit, Indian Institute of Science, Bangalore 560 012, India

[†]Central Electrochemical Research Institute, Karaikudi 630 006, India

MS received 24 May 2006

Abstract. Cubic fluorite related $\text{Bi}_{1-x}\text{Ln}_x\text{O}_{1.5}$ ($\text{Ln} = \text{Y}$ and La–Yb) phases are synthesized by solution-combustion method using glycine as the fuel. The cubic fluorite phase is stabilized with 25 mole% of rare earth cations. The lattice parameter of cubic phase increases linearly with size of the lanthanide ion. The synthesized powders are nano-metric in size and exhibit excellent compactability and reach 98% densification even on short period of sintering. The oxides with relatively larger cations Nd, Sm, Eu, Pr and Gd with 25 mole% composition transform to rhombohedral structure while others retain cubic upon sintering. All the phases show high oxide-ion conductivity and the values obtained are in good agreement with the reported values.

Keywords. Combustion synthesis; bismuth oxides; oxide-ion conductors.

1. Introduction

Cubic $\text{Bi}_{1-x}\text{Ln}_x\text{O}_{1.5}$ ($\text{Ln} = \text{Y}$ and La–Yb) phases are known to be good oxide-ion conductors (Takahashi *et al* 1972; Shuk *et al* 1996; Sammes *et al* 1999) with their application as electrolytes in solid oxide fuel cells (Tedson *et al* 1969), oxygen sensors (Adamian *et al* 1996), and pigments (Gonzalvo *et al* 2001). $d\text{-Bi}_2\text{O}_3$ crystallizes in fluorite related structure and it is stable in the temperature region 730–825°C (Takahashi and Iwahara 1978). $d\text{-Bi}_2\text{O}_3$ is stabilized at room temperature by the substitution of Ln^{3+} ions (Rao *et al* 1969; Iwahara *et al* 1981). Different models have been proposed to explain oxide-ion conductivity in $d\text{-Bi}_2\text{O}_3$ and rare-earths stabilized cubic Bi_2O_3 systems (Verkerk *et al* 1981; Kilner and Faktor 1983; Jacobs and Mac Donnell 1987). According to Mairesse (1993), the oxide-ion conductivity in these materials arises due to: (i) 1/4 of the oxide ion vacancies being accommodated in the fluorite-type lattice, (ii) the $6s^2$ lone pair electrons present in Bi^{3+} influence the polarizability of the oxide-ion network which would facilitate the oxide-ion mobility and (iii) the ability of the Bi^{3+} to accommodate highly disordered surroundings. The extent of disorder in the $d\text{-Bi}_2\text{O}_3$ structure increases with increasing temperature.

In general, the rare-earth stabilized $d\text{-Bi}_2\text{O}_3$ systems are prepared by a conventional solid-state reaction between Bi_2O_3 and Ln_2O_3 at about 800°C for several hours with repeated grinding steps (Li *et al* 1999). Other methods

such as sol-gel (Joshi and Krupanidhi 1992), co-precipitation (Kruidhof *et al* 1987) and micro-emulsion (Bhattacharya and Mallick 1994) have also been used to synthesize $\text{Bi}_2\text{O}_3\text{–Ln}_2\text{O}_3$ solid solutions. These synthetic methods have an advantage over the solid state methods in terms of homogeneity and small size particles with high surface area products. However, sol-gel method needs expensive raw materials. It also takes longer time for preparation, because of several steps involved in the process. Solution combustion method has been successfully practiced to make oxide materials (Patil *et al* 1997). Pure oxide solid solutions in nanometric size can be made by this method. In this paper, we report the single-step, solution combustion synthesis of $\text{Bi}_{1-x}\text{Ln}_x\text{O}_{1.5}$ phases, which have excellent densification and exhibit high oxide-ion conductivity.

2. Experimental

The powder samples of $\text{Bi}_{1-x}\text{Ln}_x\text{O}_{1.5}$ phases were prepared by solution combustion method using corresponding metal nitrates and glycine. General synthetic procedure followed was as follows. Stoichiometric amount of bismuth nitrate and a rare earth oxide (preheated to 850°C), were dissolved in minimum required amount of HNO_3 in a cylindrical pyrex dish and the resulting solution was heated on a hot plate to minimize the total volume of liquid to about 10–15 ml. To the resulting mixed metal nitrates solution a stoichiometric amount of glycine was added. The glycine dissolved and formed a clear solution which was introduced into a muffle furnace preheated to 400°C. The mixture boiled, followed by frothing and ignited with

*Author for correspondence (mshegde@sscu.iisc.ernet.in)

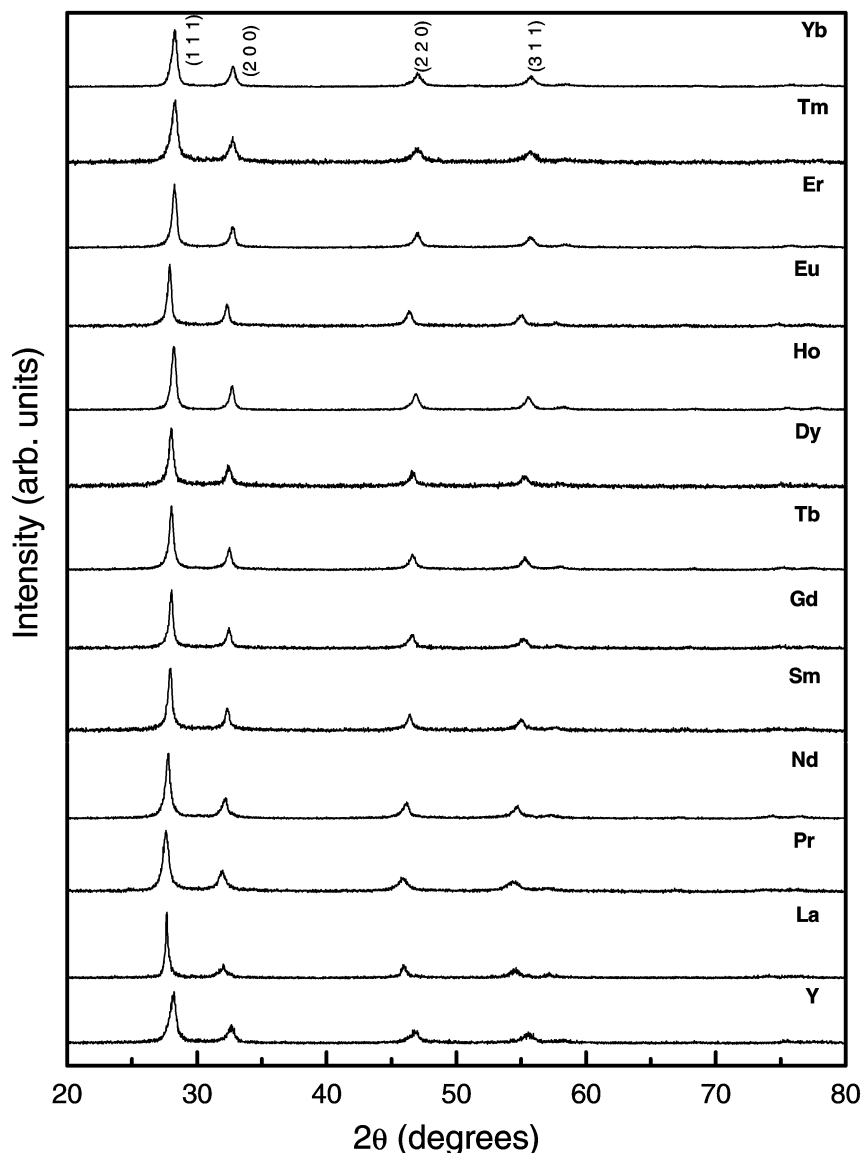
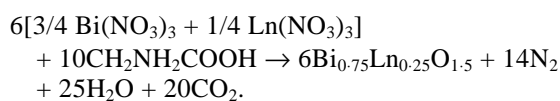


Figure 1. Powder X-ray diffraction patterns for as synthesized $\text{Bi}_{1-x}\text{Ln}_x\text{O}_{1.5}$ ($\text{Ln} = \text{La}, \text{Pr}, \text{Nd}, \text{Sm}, \text{Eu}, \text{Gd}, \text{Tb}, \text{Dy}, \text{Ho}, \text{Er}, \text{Tm}, \text{Yb}$ and Y) phases.

evolution of large amount of gases. The flame persisted for about a minute leaving behind a residual yellow coloured powder. With less than 3 g of total metal nitrates, the reactions were found to be highly controlled and safe. The value of 'x' for all the samples of $\text{Bi}_{1-x}\text{Ln}_x\text{O}_{1.5}$ compositions was kept constant at 0.25 except for La whose value was 0.12.

The combustion synthesis reaction occurred as follows:



All the samples studied here were characterized by powder X-ray diffraction (XRD) using Philips X'pert Pro diffracto-

meter with CuK_α ($\lambda = 1.5418 \text{ \AA}$) using graphite monochromator to filter the K_β lines. Data were collected at a scan rate of $1^\circ/\text{min}$ with a 0.02° step size for 2θ from 20 – 80° . Morphology and compositional analysis were carried out in the scanning electron microscope (SEM). Ionic conductivity measurements were carried out on pellets of 10 mm diameter and ~ 2 mm thickness which were obtained by applying isostatic pressure of 25 Mpa sintered at 750°C for 12 h. The flat pellet surfaces were coated with gold paste which served as electrodes for measurements. Impedance data were obtained over the frequency range 100–15 MHz between room temperature and 700°C employing a HP4194A Impedance/Gain-Phase Analyser interfaced with an IBM-PC in flowing dry air. The samples were equilibrated for about 2 h prior to each measurement.

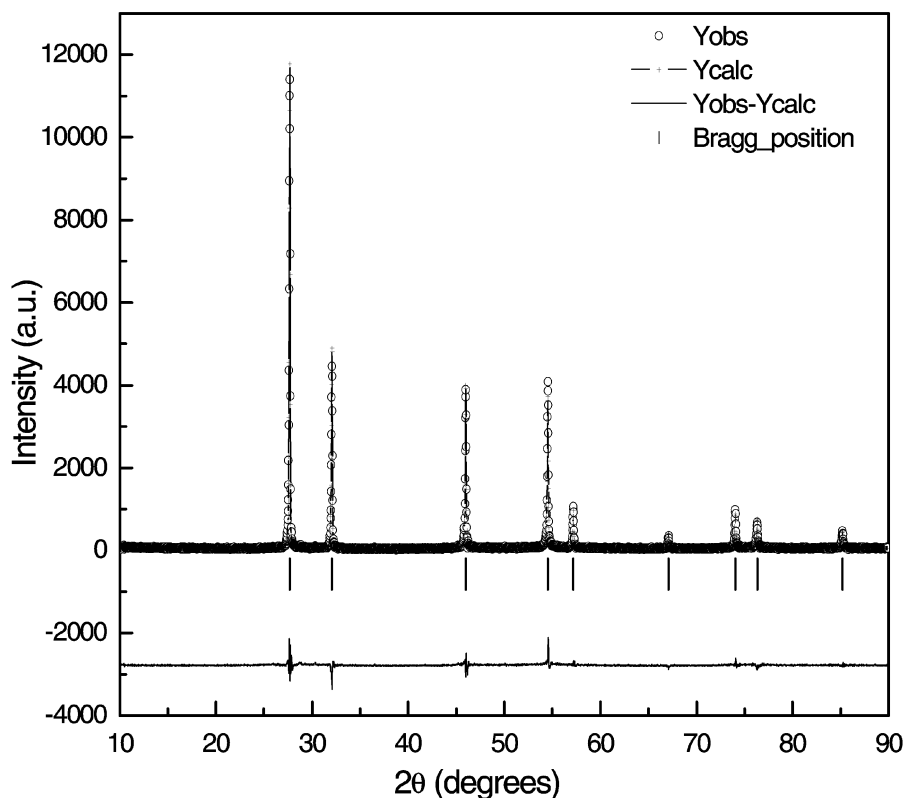


Figure 2. Rietveld refined X-ray diffraction patterns for $\text{Bi}_{0.88}\text{La}_{0.12}\text{O}_{1.5}$ phase showing good fitting of observed (o), calculated (solid line), difference pattern (bottom) and Bragg positions (vertical bars).

Table 1. The lattice parameter, ionic size, crystallite size calculated from the line broadening using Scherrer equation and surface areas of $\text{Bi}_{1-x}\text{Ln}_x\text{O}_{1.5}$ phases.

Compound	Ionic radii of Ln^{3+} (pm)	Lattice parameter, a (Å)	Average crystallite size (nm)	BET surface area (m^2/g)
$\text{Bi}_{0.75}\text{Yb}_{0.25}\text{O}_{1.5}$	100.8	5.4733	13.82	10.17
$\text{Bi}_{0.75}\text{Tm}_{0.25}\text{O}_{1.5}$	102.0	5.4763	10.77	12.63
$\text{Bi}_{0.75}\text{Er}_{0.25}\text{O}_{1.5}$	103.0	5.4766	14.40	14.09
$\text{Bi}_{0.75}\text{Y}_{0.25}\text{O}_{1.5}$	104.0	5.4895	10.85	29.54
$\text{Bi}_{0.75}\text{Ho}_{0.25}\text{O}_{1.5}$	104.1	5.4911	15.60	12.78
$\text{Bi}_{0.75}\text{Dy}_{0.25}\text{O}_{1.5}$	105.2	5.5129	14.13	13.94
$\text{Bi}_{0.75}\text{Tb}_{0.25}\text{O}_{1.5}$	106.3	5.5027	15.38	18.80
$\text{Bi}_{0.75}\text{Gd}_{0.25}\text{O}_{1.5}$	107.8	5.5174	16.68	11.30
$\text{Bi}_{0.75}\text{Eu}_{0.25}\text{O}_{1.5}$	108.7	5.5260	17.25	12.29
$\text{Bi}_{0.75}\text{Sm}_{0.25}\text{O}_{1.5}$	109.8	5.5371	15.51	13.51
$\text{Bi}_{0.75}\text{Nd}_{0.25}\text{O}_{1.5}$	112.3	5.5685	12.96	13.78
$\text{Bi}_{0.75}\text{Pr}_{0.25}\text{O}_{1.5}$	113.0	5.5579	11.87	14.17
$\text{Bi}_{0.88}\text{La}_{0.12}\text{O}_{1.5}$	117.2	5.5773	20.62	9.20

Electrical conductivity of various $\text{Bi}_{1-x}\text{Ln}_x\text{O}_{1.5}$ was determined from their complex-impedance plot. The structures were refined by Rietveld method using room temperature powder X-ray data.

3. Results and discussion

Figure 1 shows the powder XRD patterns of as-prepared $\text{Bi}_{1-x}\text{Ln}_x\text{O}_{1.5}$ ($\text{Ln} = \text{Y}, \text{La}-\text{Yb}$) oxides. Extent of lanthanide

substitution was 25 mole% ($x = 0.25$), except for La ($x = 0.12$). As synthesized oxides crystallize in cubic fluorite structure. The structural parameters are obtained from the Rietveld refinement method using Fullprof suite programme. A typical refined pattern for $\text{Bi}_{0.88}\text{La}_{0.12}\text{O}_{1.5}$ is shown in figure 2. In all the cases the observed intensities fit well with the model and the lattice parameters obtained are in good agreement with the reported values for the same composition. The lattice parameters and ionic size of Ln^{3+} ion are summarized along with crystallite size and

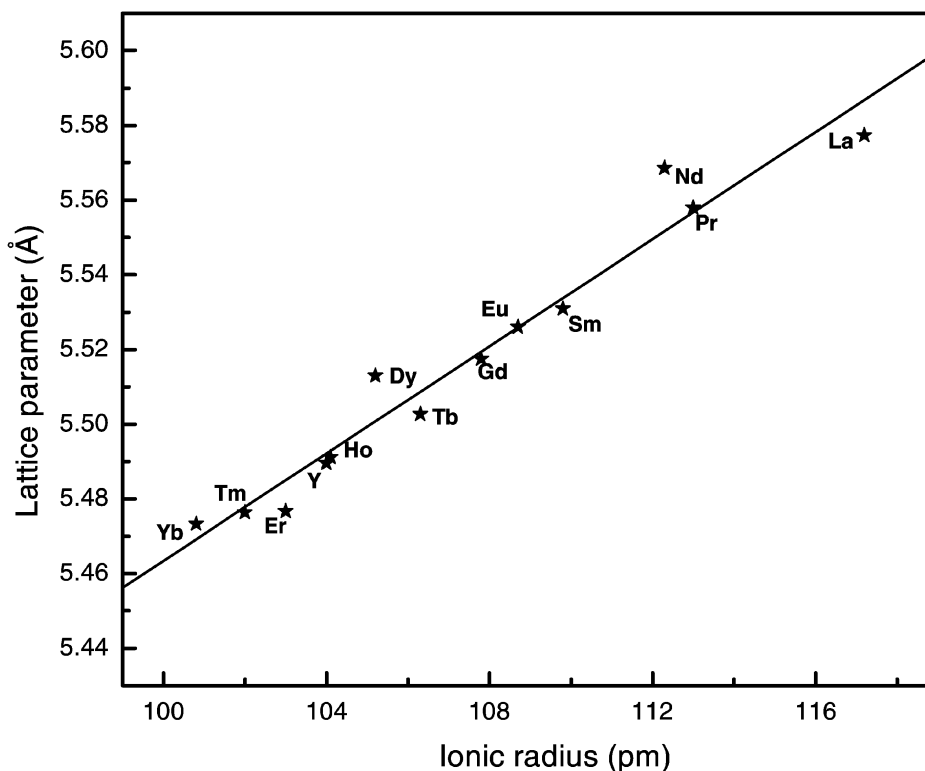


Figure 3. Evolution in cubic cell parameters for the $\text{Bi}_{1-x}\text{Ln}_x\text{O}_{1.5}$ phases within its cubic domain of stability ($x = 0.25$ except for La whose value is 0.12).

Table 2. The lattice parameters for the rhombohedral phases which were obtained by quenching the cubic phases.

Compound	Lattice parameter (Å)		
	<i>a</i>	<i>b</i>	<i>c</i>
$\text{Bi}_{0.75}\text{Pr}_{0.25}\text{O}_{1.5}$	4.033	4.033	27.609
$\text{Bi}_{0.75}\text{Nd}_{0.25}\text{O}_{1.5}$	3.998	3.998	27.535
$\text{Bi}_{0.75}\text{Sm}_{0.25}\text{O}_{1.5}$	3.976	3.976	27.357
$\text{Bi}_{0.75}\text{Eu}_{0.25}\text{O}_{1.5}$	3.964	3.964	27.311
$\text{Bi}_{0.75}\text{Gd}_{0.25}\text{O}_{1.5}$	3.961	3.961	27.291

BET surface areas in table 1. The plot of ionic radius vs 'a' parameter is shown in figure 3. The 'a' parameter varies linearly with ionic radius of the rare earth ions.

For conductivity measurements the powder sample was pelletized and sintered at 750°C for 12 h followed by quenching to room temperature to retain cubic phase of $\text{Bi}_{1-x}\text{Ln}_x\text{O}_{1.5}$. It is found that the samples with $x = 0.25$ for relatively larger Ln^{3+} ions ($\text{Ln} = \text{Pr}, \text{Nd}, \text{Sm}, \text{Eu}$ and Gd) transformed to rhombohedral phases even on quenching. However, for larger ion, La with the same composition ($x = 0.25$) crystallizes in rhombohedral structure and the cubic fluorite phase is stabilized with lower concentration, $x = 0.12$. In the present investigation, the samples with a

small cation radius such as Y^{3+} stabilizes cubic fluorite type structure and is stable over a wide range of temperatures. In figure 4, we have shown XRD pattern of quenched sample. All the diffracted lines indexed to rhombohedral cell with hexagonal setting. The lattice parameters agree well with the reported values (Hirano and Namikawa 1999; Drache *et al* 1999). The cell parameters are summarized in table 2.

All the as prepared powders irrespective of the phases formed are agglomerates of smaller crystallites which were evident from the scanning electron micrograph presented in figure 5(a) for a representative sample, $\text{Bi}_{0.88}\text{La}_{0.12}\text{O}_{1.5}$. These powders show high compactability even with lower sintering temperature and time. The pellets uniformly pressed at 25 Mpa sintered at 750°C for 12 h show 98% density. The SEM image of a pellet illustrated in figure 5(b) shows microstructure of the pellet. The sintering at 750°C leads to a grain growth of small size particles.

The a.c. impedance measurements performed on the sintered pellets showed excellent ionic conductivity. The oxide ion conductivity values obtained in air for the sintered pellets of $\text{Bi}_{1-x}\text{Ln}_x\text{O}_{1.5}$ phases are summarized in table 3. The conductivity values for similar compositions and temperature are compared with the reported values (Shuk *et al* 1996). Corresponding Arrhenius plots of conductivity are shown in figure 6. The Arrhenius plots showed linear relation over the whole range of temperatures

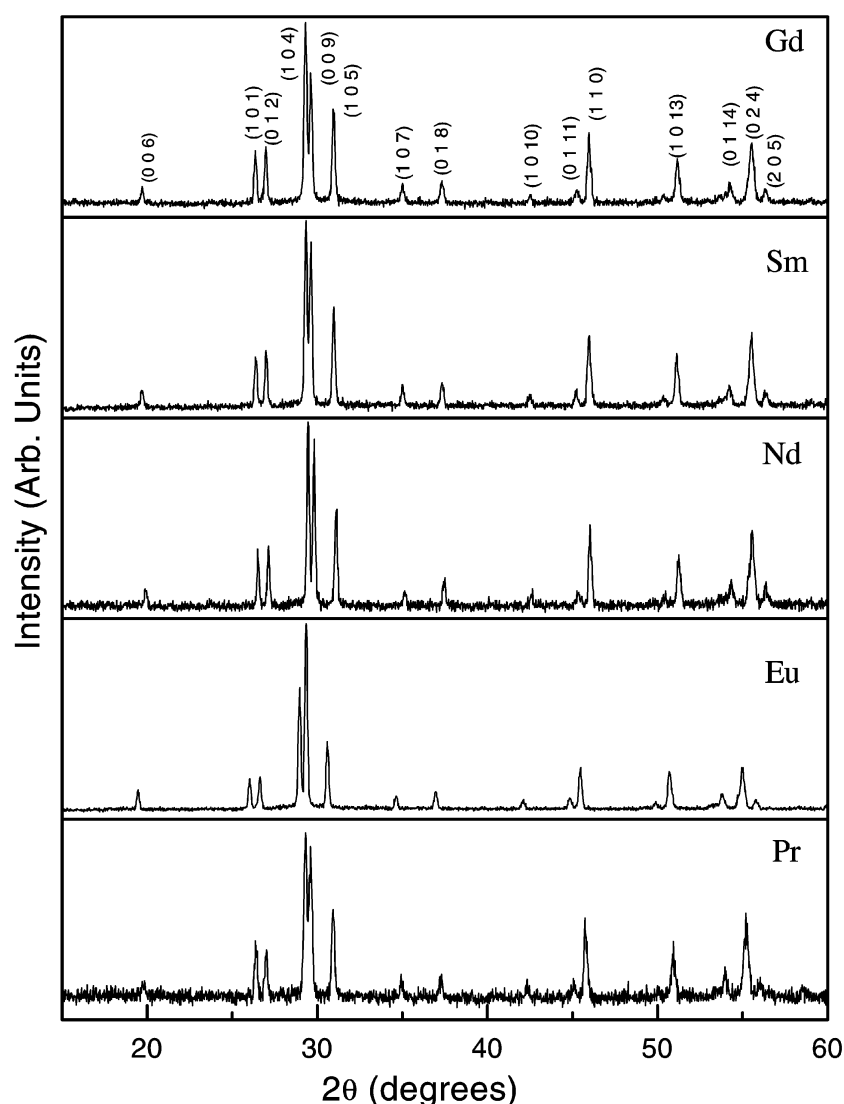


Figure 4. X-ray diffraction patterns for $\text{Bi}_{1-x}\text{Ln}_x\text{O}_{1.5}$ ($\text{Ln} = \text{Gd}, \text{Sm}, \text{Nd}, \text{Eu}$ and Pr) phases heated in air at a heating rate of $6^\circ/\text{min}$ up to 800°C and quenched to ambient temperature.

Table 3. Conductivity values at different temperatures along with their activation energies obtained for $\text{Bi}_{1-x}\text{Ln}_x\text{O}_{1.5}$ phases.

Compounds	Conductivity ($\text{ohm}^{-1} \text{cm}^{-1}$)					E_a (eV)
	Experimental			Literature		
	500°C	650°C	700°C	500°C	650°C	
$\text{Bi}_{0.75}\text{Yb}_{0.25}\text{O}_{1.5}$	8.40×10^{-4}	2.50×10^{-2}	5.00×10^{-3}	8.30×10^{-3}	7.4×10^{-2}	0.53
$\text{Bi}_{0.75}\text{Tm}_{0.25}\text{O}_{1.5}$	3.57×10^{-3}	—	—	7.0×10^{-3}	8.0×10^{-2}	0.54
$\text{Bi}_{0.75}\text{Er}_{0.25}\text{O}_{1.5}$	3.47×10^{-3}	—	—	1.27×10^{-2}	1.35×10^{-1}	0.46
$\text{Bi}_{0.75}\text{Y}_{0.25}\text{O}_{1.5}$	6.25×10^{-3}	—	—	1.30×10^{-2}	1.10×10^{-2}	0.62
$\text{Bi}_{0.75}\text{Ho}_{0.25}\text{O}_{1.5}$	5.00×10^{-3}	—	—	1.35×10^{-2}	1.70×10^{-1}	0.49
$\text{Bi}_{0.75}\text{Dy}_{0.25}\text{O}_{1.5}$	4.20×10^{-3}	—	—	1.35×10^{-2}	1.20×10^{-1}	0.54
$\text{Bi}_{0.75}\text{Tb}_{0.25}\text{O}_{1.5}$	5.00×10^{-3}	3.13×10^{-2}	4.03×10^{-2}	3.40×10^{-3}	1.20×10^{-2}	0.71
$\text{Bi}_{0.75}\text{Gd}_{0.25}\text{O}_{1.5}$	8.33×10^{-5}	2.50×10^{-3}	7.81×10^{-3}	3.5×10^{-3}	5.6×10^{-2}	0.52
$\text{Bi}_{0.75}\text{Eu}_{0.25}\text{O}_{1.5}$	4.76×10^{-4}	1.67×10^{-3}	1.67×10^{-2}	—	—	0.51
$\text{Bi}_{0.75}\text{Sm}_{0.25}\text{O}_{1.5}$	1.25×10^{-3}	1.70×10^{-2}	2.50×10^{-2}	2.3×10^{-3}	2.0×10^{-2}	0.48
$\text{Bi}_{0.75}\text{Nd}_{0.25}\text{O}_{1.5}$	8.33×10^{-3}	2.50×10^{-2}	—	—	—	0.46
$\text{Bi}_{0.75}\text{Pr}_{0.25}\text{O}_{1.5}$	5.00×10^{-3}	4.16×10^{-2}	7.30×10^{-2}	3.0×10^{-3}	2.0×10^{-2}	0.47
$\text{Bi}_{0.88}\text{La}_{0.12}\text{O}_{1.5}$	1.00×10^{-3}	8.93×10^{-3}	5.00×10^{-2}	—	—	0.45

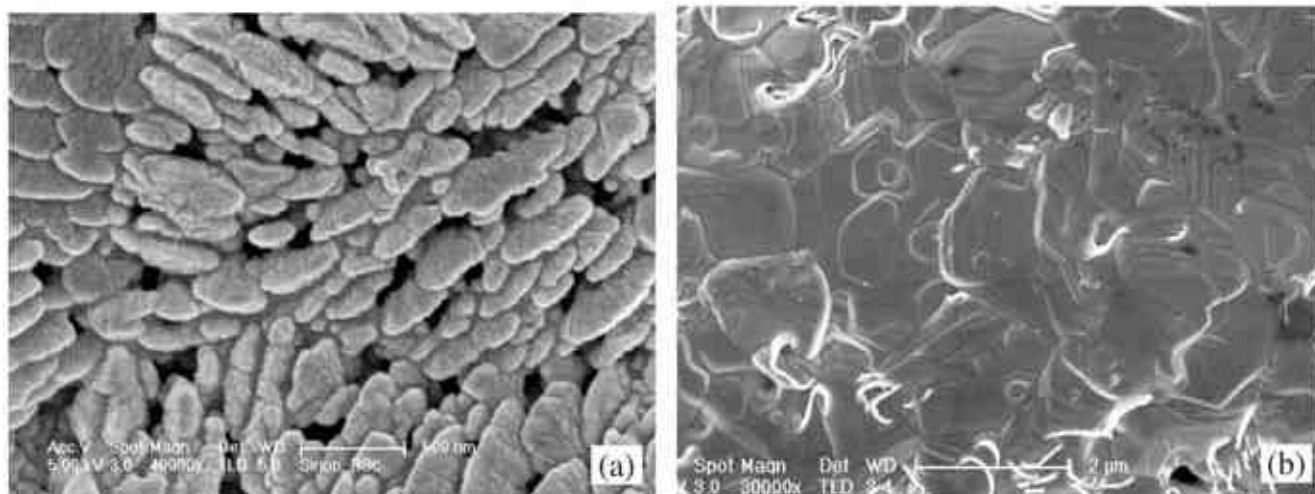


Figure 5. Scanning electron micrographs of (a) as-prepared $\text{Bi}_{0.75}\text{Y}_{0.25}\text{O}_{1.5}$ and (b) pellet sintered at 800°C .

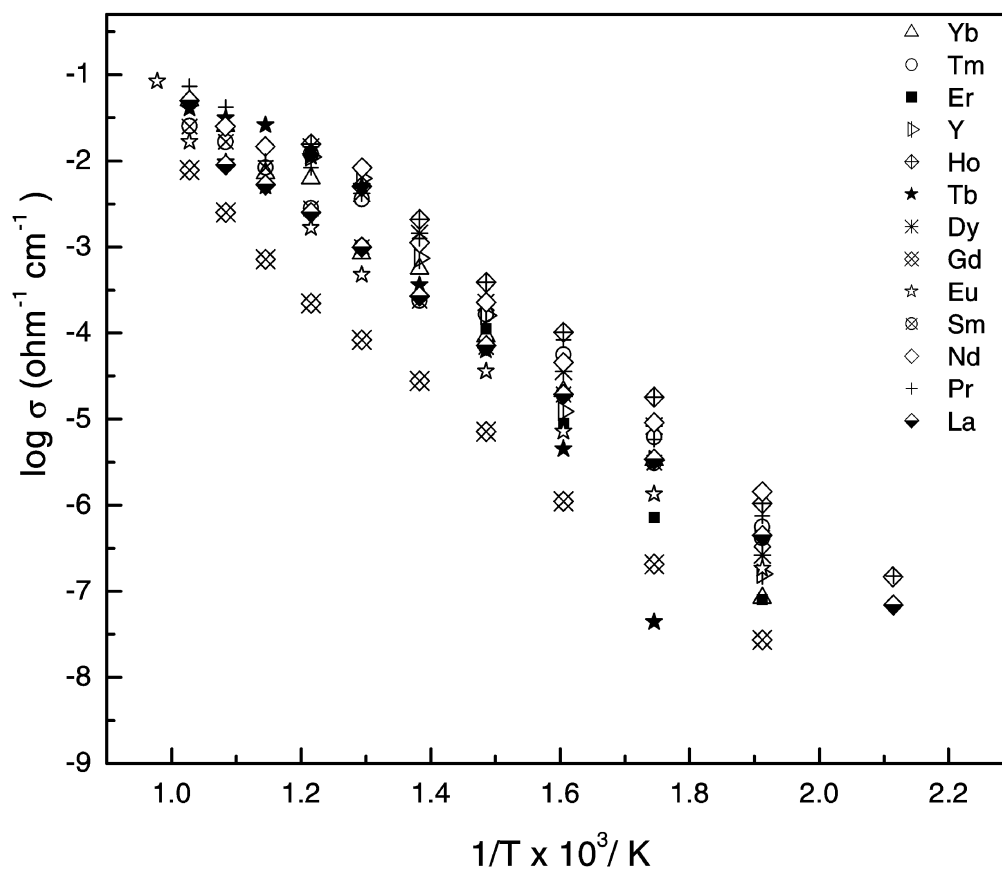


Figure 6. Conductivity vs temperature plots for the sintered pellets of $\text{Bi}_{1-x}\text{Ln}_x\text{O}_{1.5}$ ($\text{Ln} = \text{La}, \text{Pr}, \text{Nd}, \text{Sm}, \text{Eu}, \text{Gd}, \text{Tb}, \text{Dy}, \text{Ho}, \text{Er}, \text{Tm}, \text{Yb}$ and Y) phases.

measured irrespective of cubic or rhombohedral phases. As can be seen, the ionic conductivity observed over the combustion synthesized material, agrees well with the reported values in the literature.

4. Conclusions

In conclusion, $\text{Bi}_{1-x}\text{Ln}_x\text{O}_{1.5}$ ($\text{Ln} = \text{Y}$ and $\text{La}-\text{Yb}$) phases, were synthesized by solution combustion method. The

lattice constant monotonically increases with increasing ionic radii of the rare earth ions. The nanosize particles obtained by this method can be easily sintered at 700°C for 12 h giving 98% densification. Ionic conductivity of these oxides compare well with those reported in the literature.

Acknowledgements

The authors thank Prof. K C Patil, Inorganic and Physical Chemistry, IISc, Bangalore, for helpful discussion. Financial assistance from the Department of Science and Technology, Government of India, is gratefully acknowledged.

References

- Adamian Z N, Abovian H V and Aroutiounian V M 1996 *Sensors & Actuators Part B: Chem.* **35** 241
- Bhattacharya A K and Mallick K K 1994 *Solid State Commun.* **91** 357
- Drache M, Obbade S, Wignacourt J P and Conflant P 1999 *J. Solid State Chem.* **142** 349
- Gonzalvo B, Romero J, Fernández F and Torralvo M J 2001 *J. Alloys & Compos.* **323** 372
- Hirano T and Namikawa T 1999 *IEEE Trans. Magn.* **35** 3487
- Iwahara H, Esaka T, Sato T and Takahashi T 1981 *J. Solid State Chem.* **39** 173
- Jacobs P W M and Mac Donnell D A 1987 *Solid State Ionics* **23** 295
- Joshi P C and Krupanidhi S B 1992 *J. Appl. Phys.* **72** 5827
- Kilner J A and Faktor J D 1983 in *Prog. solid electrolytes* (eds) T A Wheat *et al* (Ottawa: Canada Centre for Mineral and Energy Technology) p. 347
- Kruidhof H, Seshan Jr. K, Lippens B C, Gellings P J and Burggraaf A J 1987 *Mater. Res. Bull.* **22** 1635
- Li W Q, Li J, Xia X and Chao Y L 1999 *Acta Chim. Sin.* **57** 491
- Mairesse G 1993 in *Fast ion transport in solids* (ed.) B Scrosati (Amsterdam: Kluwer) p. 271
- Patil K C, Aruna S T and Ekambaram S 1997 *Current Opinion in Solid State and Mater. Sci.* **2** 158
- Rao C N R, Subba Rao G V and Ramdas S 1969 *J. Phys. Chem.* **73** 672
- Sammes N M, Tompsett G A, Näfe H and Aldinger F 1999 *J. Eur. Ceram. Soc.* **19** 1801
- Shuk P, Wiemhöfer H-D, Guth U, Göpel W and Greenblatt M 1996 *Solid State Ionics* **89** 179
- Takahashi T and Iwahara H 1978 *Mater. Res. Bull.* **13** 1447
- Takahashi T, Iwahara H and Nagai Y 1972 *J. Electrochem. Soc.* **119** 97
- Tedson C S, Spacil Jr H S and Mitoff S P 1969 *J. Electrochem. Soc.* **116** 1170
- Verkerk M J and Burggraaf A J 1981 *Solid State Ionics* **3/4** 463